Available online at www.sciencedirect.com
SCIENCE DIRECT
Polymer 46 (2005) 4789–4798
polymer
www.elsevier.com/locate/polymer

Thermal, optical, electrochemical properties and conductivity of *trans*- and *cis*-poly(1-ethynylpyrene): a comparative investigation

Ernesto Rivera[a,*], Martha Aguilar-Martínez[b], Gerardo Terán[a], Raúl F. Flores[a], José Antonio Bautista-Martínez[b]

[a]*Instituto de Investigaciones en Materiales UNAM, Circuito Exterior Ciudad Universitaria C.P., 04510 México, DF, México*
[b]*División de Estudios de Posgrado Facultad de Química UNAM, Departamento de Fisicoquímica, Ciudad Universitaria C.P., 04510 México, DF, México*

Received 17 November 2004; received in revised form 22 March 2005; accepted 1 April 2005
Available online 21 April 2005

Abstract

The thermal, optical and electrochemical properties of *trans*-poly(1-ethynylpyrene) (*trans*-PEP) and *cis*-poly(1-ethynylpyrene) (*cis*-PEP) have been studied as a function of polymer backbone configuration and internal stacking. Absorption spectra of the polymers showed that *trans*-PEP possesses a higher degree of conjugation than its homologue, *cis*-PEP. Intramolecular interactions occur between adjacent pendant pyrene units (associated pyrenes) present in each polymer, giving rise to static excimer emissions, strongest in *cis*-PEP because of the shorter distances between aromatic rings. Data resulting from excitation spectra and fluorescence decay profiles proved that such interactions take place in the ground state. Cyclic voltammetry of *trans*- and *cis*-PEP exhibited irreversible behaviors with different oxidation potentials as a result of their dissimilar geometry.

Keywords: Poly(1-ethynylpyrene); Optical properties; Electrochemistry

1. Introduction

Over the last 30 years, π-conjugated polymers have been regarded as promising materials for the development of electronic devices such as light emitting diodes, photovoltaic cells and non-linear optical systems [1–5]. The optoelectronic properties vary remarkably depending on the degree of conjugation length between the consecutive repeat units. Although polyacetylene is a highly conjugated polymer and shows metallic conductivity upon doping, its insolubility, instability as well as its improcessability, limits its practical applications as a functional material [6]. The introduction of alkyl or aryl substituents on the polyacetylene backbone significantly improves its stability but tends to decrease the degree of conjugation due to increased torsions, which skew the polymer backbone's planarity [7–10].

Polyarylacetylenes (particularly polyphenylacetylene) have been widely studied by many research groups [11]. In general, polyarylacetylenes exhibit *trans*-transoidal, *cis*-transoidal, *trans*-cisoidal and *cis*-cisoidal geometries as shown in studies involving FTIR and ^{1}H NMR investigations of polyphenylacetylene [12,13].

Arylacetylenes bearing non-polar groups are usually polymerized in the presence of WCl_6 and disubstituted acetylenes are usually polymerized in the presence of $TaCl_5$ [14]. Masuda and co-workers reported the polymerization of several arylcetylenes bearing bulky condensed aromatic rings, [15,16] and obtained polymers with molecular weights up to 140,000 g/mol depending on the structure of the monomer. Surprisingly, many of these polymers were shown to be highly conjugated despite increased steric effects. The position of the acetylene bond in the aromatic ring significantly influences the reactivity of the monomer towards polymerization due to steric and electronic effects [15]. Nevertheless, arylacetylenes bearing polar groups such as –CN, –OR, –SR, –NR and –N=N– cannot be polymerized with WCl_6 [17] but they can be polymerized by the employment of other catalytic systems [17–20].

In the present work, we have studied the dependency of

* Corresponding author. Tel.: +52 55 56 22 47 33; fax: +52 55 56 16 12 01.
E-mail address: riverage@zinalco.iimatercu.unam.mx (E. Rivera).

0032-3861/$ - see front matter © 2005 Elsevier Ltd. All rights reserved.
doi:10.1016/j.polymer.2005.04.003

thermal, optical and electrochemical properties of polyarylacetylenes bearing condensed aromatic groups on the geometry of the polyacetylene backbone and the internal stacking of pendant substituents.

For this purpose, we selected poly(1-ethynylpyrene) as model molecule because the pyrene unit is an efficient fluorescent probe, which has been successfully used as a molecular label in the study of many polymers [21–30]. It is well known that pyrene has a long singlet lifetime and that it readily forms excimers; the relevant photophysical properties of pyrene have recently been reviewed [31].

In a previous work [32], we reported the polymerization of 1-ethynylpyrene (EP) and other related monomers under different reaction conditions; the preparation of *trans*-PEP and *cis*-PEP is shown in Fig. 1. Catalytic polymerization of EP with WCl_6 resulted in the formation of *trans*-PEP with molecular weights ranging from 24,000 to 470,000 g/mol and polydispersities between 2.9 and 11 [32]. These dark purple polymers were totally soluble in *o*-dichlorobenzene, very soluble in THF and partially soluble in toluene and $CHCl_3$. On the other hand, EP was also polymerized in the presence of $Rh_2nbd_2Cl_2$ to give a *cis*-cisoidal poly (1-ethynylpyrene) [16]. This dark brown polymer was practically insoluble in all common organic solvents [15]. According to the literature, *cis*-cisoidal polyarylacetylenes usually have a poor solubility in organic solvents making them sometimes difficult to characterize by common analytical methods. However, Tabata and co-workers used resonance Raman spectroscopy to confirm the *cis*-cisoidal nature of poly(1-naphtylacetylene) [34].

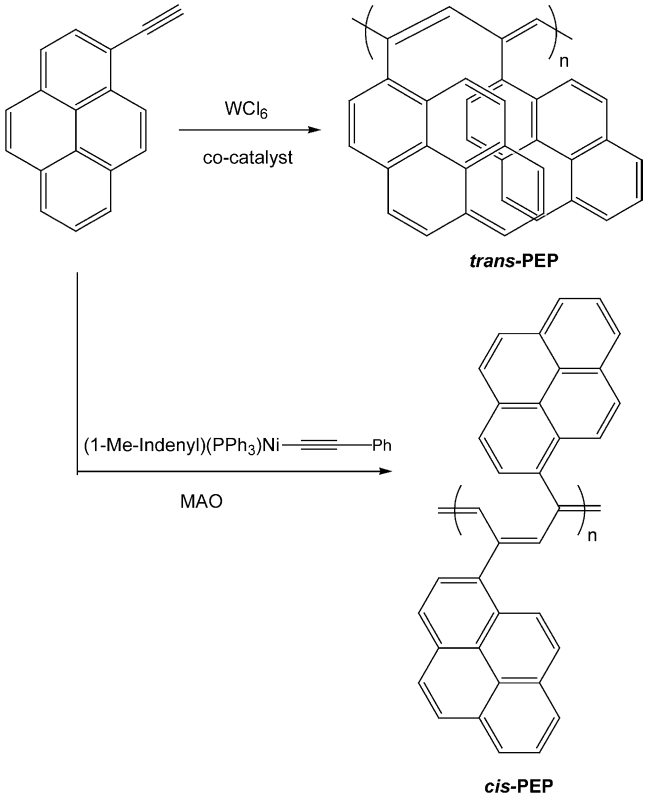

Fig. 1. Polymerization of 1-ethynylpyrene with different catalysts.

Previously, we studied superficially the optical properties of these polymers as a function of main chain geometry [36]. However, to get a deeper insight into the effect of the stacking, we studied three new geometrically different di (1-ethynylpyrene) derivatives by UV–vis and Fluorescence spectroscopy for comparison with their respective polymers [37]. In the other studies, we also carried out the polymerization of EP using the catalytic system developed by Zargarian and co-workers: (1-Me-Indenyl)(PPh_3)Ni–C≡C–Ph and methylaluminoxane (MAO), (named here NiC/MAO) [35]. This method provided the formation of soluble *cis*-transoidal polymers (*cis*-PEPs, Fig. 1) with molecular weights from $M_w = 2200$ to 24,000 g/mol and polydispersities of about $M_w/M_n \approx 2$ [33]. The *cis*-polymers were dark brown, very soluble in *o*-dichlorobenzene, fairly soluble in THF and poorly soluble in $CHCl_3$. Since, the properties of polyarylacetylenes have a large dependence on the geometry of the polyacetylene backbone, we decided to carry out a comparative study between *trans*-PEP synthesized with WCl_6 and *cis*-PEP obtained with NiC/MAO, bearing identical molecular weights ($M_w = 24{,}000$ g/mol). Finally, the electrochemical properties of EP, *trans*-PEP and *cis*-PEP were studied and their conductivities were measured in pressed pellet.

2. Experimental section

The synthesis and characterization of *trans*-PEP [32] and *cis*-PEP [33] was achieved according to our previously published procedures. Two samples of these polymers having identical molecular weights ($M_w = 24{,}000$ g/mol) were selected for this investigation. Di(1-ethynylpyrene) derivatives (DEP): *syn*-1,3-di(1-pyrenyl)-1,3-butadiene (DEPS), *anti*-1,3-di(1-pyrenyl)-1,3-butadiene (DEPA) and 2,4-di(1-pyrenyl)-1-butene (DEPH) (Fig. 2) were also previously synthesized and characterized by us [37].

Thermal properties of the polymers were studied by determining T_{10} (10% weight loss temperature), T_g (glass transition temperature), and T_m (melting point). Thermogravimetric analysis (TGA) was conducted on a Hi-Res TGA 2950 Instrument (from 20 to 1000 °C) and differential scanning calorimetry (DSC) was carried out on a DSC 2910 instrument (from −40 to 400 °C), in both cases with a heating rate of 20 °C/min.

For UV–vis and fluorescence spectroscopies, tetrahydrofuran (THF) was purchased from Aldrich (spectrophotometric grade). Prior to use, the solvent was checked for spurious emission in the region of interest and found to be satisfactory. The absorption spectra in solution and in the solid state (film cast from THF solution) were recorded on a Varian Cary 1 Bio UV/vis spectrophotometer (model 8452A) using 1 cm quartz cells and solute concentrations of $1–3 \times 10^{-5}$ M for both the polymers and the dimers. It

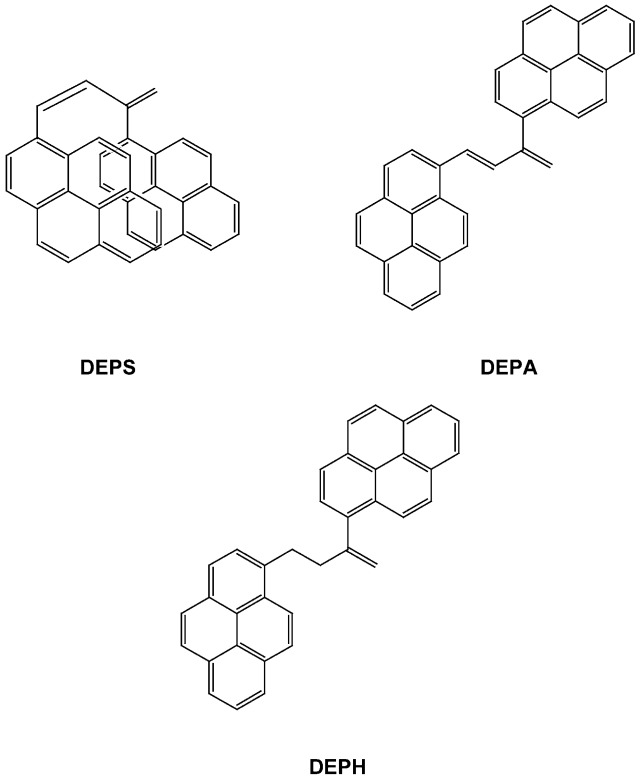

Fig. 2. Structures of DEPS, DEPA and DEPH.

has been verified that the Beer–Lambert law applies for the concentrations used. Fluorescence spectra corrected for the emission detection were recorded on a Spex Fluorolog-2 spectrophotometer with an F2T11 special configuration. Each solution was excited near the absorption wavelength maximum using a 1 cm quartz cell. For polymers and dimers a concentration of about $1–3\times10^{-6}$ M was used giving absorbances of less than 0.1 in order to avoid any inner filter effect.

Fluorescence lifetimes were measured on a multiplexed time-correlated single photon counting fluorometer (Edinburgh Instruments, model 299T). The instrument incorporates an all-metal coaxial hydrogen flashlamp. Reconvolution analysis was performed by fitting over the entire fluorescence decay including the rising edge. The kinetic interpretation of the goodness-of-fit was assessed using plots of weighted residuals, the reduced χ^2 value, and Durbin–Watson (DW) parameters. The lifetime measurements were performed in argon-saturated solutions of the substrates at room temperature. Intensity ratios for the dimers (I_M/I_E) were calculated dividing the relative intensity of the monomer band (I_M) by the relative intensity of the excimer band (I_E). Where I_M and I_E were measured at $\lambda_M=$ 402 nm and $\lambda_E=480$ nm for DEPS, and at $\lambda_M=390$ nm and $\lambda_E=493$ nm for DEPA.

THF (spectrophotometric grade, Aldrich) was used as solvent for the electrochemical procedures and tetra *n*-butylammonium perchlorate (*n*-Bu_4NClO_4) (Fluka), dried at 60 °C under vacuum for 24 h prior to use, was employed as a supporting electrolyte. Cyclic voltammetry measurements were carried out in a conventional three-electrode cell. A polished Pt-disk electrode with an area of 3.14 mm^2 was used as a working electrode. Prior to measurements, this electrode was cleaned and polished with 0.05 μm alumina (Buehler), wiped with water and further with acetone. The counter electrode consisted of a piece of platinum wire and the reference electrode was an Ag/AgCl electrode. The concentration of the polymer solutions varied from 0.016 to 0.021 mM depending on their solubility. Voltammetric curves were recorded using a BAS Epsilon Electroanalytical Analyzer of Bioanalytical Systems interfaced with a Dell personal computer. Measurements were carried out in a potential range from −1.5 to 2.0 V, with a scan rate of 0.01–0.1 V s^{-1}. All the solutions were purged with nitrogen prior to analysis. Conductivity of the polymers in the non-doped state was measured in pressed pellet at room temperature, using a HP4192A impedancemeter operating at a frequency from 1,000,000 to 1000 Hz.

3. Results and discussion

trans-PEP and *cis*-PEP were synthesized and fully characterized, according to the procedures previously reported in the literature [32–34]. For comparison, optical properties of three novel di(1-ethynylpyrene) derivatives (DEP): *syn*-1,3-di(1-pyrenyl)-1,3-butadiene (DEPS), *anti*-1,3-di(1-pyrenyl)-1,3-butadiene (DEPA) and 1,3-di(1-pyrenyl)-1-butene (DEPH) have been also included in this study [37]. The structures of DEPS, DEPA and DEPH are shown in Fig. 2.

3.1. Thermal properties of the polymers

Thermal properties of the polymers were determined by TGA from 20 to 1000 °C (Fig. 3) and DSC from −40 to

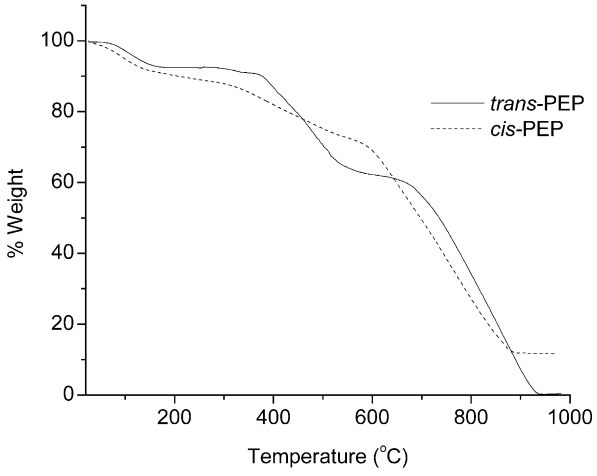

Fig. 3. TGA curves for *trans*-poly(1-ethynylpyrene) and *cis*-poly (1-ethynylpyrene).

400 °C (not shown). *trans*-PEP exhibits a T_{10} (10% weight loss temperature) of 381 °C with fast degradation in two steps, reaching 40% of weight loss at 668 °C and almost total degradation at 940 °C. On the other hand, *cis*-PEP exhibits a T_{10} of 285 °C and degrades gradually reaching 30% of weight loss at 591 °C, followed by a fast degradation step leaving 12% of the remaining mass at 887 °C. It is presumed that the slightly lower thermal stability of *cis*-PEP is attributable to relatively facile extrusion of 1-ethynylpyrene units from the *cis*-polymer backbone at elevated temperatures. Besides, *trans*-PEP exhibits a melting point at 330 °C whereas *cis*-PEP do not show either softening or melting point in the studied range of temperatures.

3.2. Optical properties of the polymers

3.2.1. Absorption spectra of trans-PEP and cis-PEP

The UV–vis spectra of *trans*-PEP and *cis*-PEP differ significantly as shown in Fig. 4 where both the solution and solid-state results are presented. Indeed, the *cis*-PEP solution spectra contain a band at 453 nm not present for *trans*-PEP, which clearly reveals the existence intramolecular interactions between adjacent pyrene pendant groups. Moreover, the band observed at 580 nm (cut off at $\lambda =$ 800 nm) in the solution absorption spectrum of *trans*-PEP is not observed for *cis*-PEP. Rather, the *cis*-PEP solution spectra exhibit a shoulder at 537 nm likely due to the associated polyacetylene backbone, suggesting a shorter effective degree of conjugation than for *trans*-PEP. Previously, molecular mechanics calculations (MM2), performed on short segments of *trans*-PEP and *cis*-PEP showed that the *trans*-PEP (Fig. 5(A)) polymer backbone is well aligned with pendant pyrene units perpendicular to the polyacetylene chain plane [33]. Pyrene groups adopt an almost parallel orientation, giving rise to regioregular stacking with pyrene–pyrene distances at about 3.1–4.5 Å. By contrast, enhanced steric interactions between pyrenes and neighboring hydrogen groups force the polyacetylene backbone to twist out of plane in *cis*-PEP (Fig. 5(B)), thereby reducing the effective conjugation length. This causes a partial non-regioregular stacking of the pendant aromatic rings so that the pendant pyrene groups of *cis*-PEP interact in a non-parallel way. Distances between pyrene units vary from 3.1 Å (near the backbone) to 4.1 Å (far from the backbone) but the lengths may increase or decrease for other pyrene pairs. Therefore, pyrene pendant groups in *trans*-PEP are well aligned and stacked, whereas the aromatic groups in *cis*-PEP are randomly oriented.

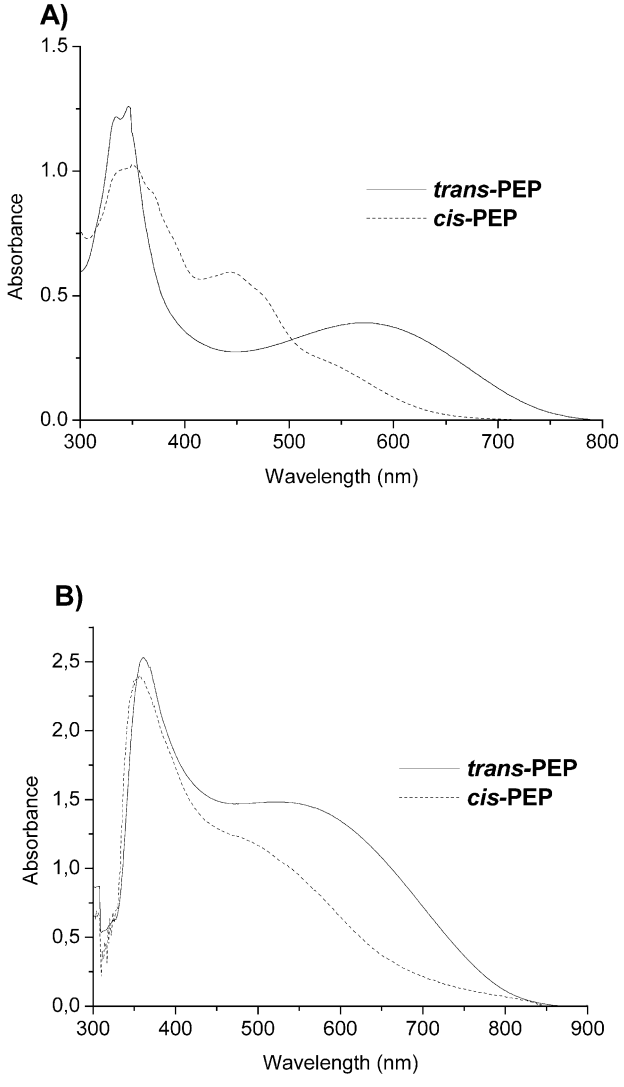

Fig. 4. Absorption spectra for *trans*- and *cis*-PEP: (A) in THF solution, (B) in casted film.

The absorption bands and absorption cutoffs of the *cis*- and *trans*-PEP spin cast films (Fig. 4(B)) exhibit a significant red shift as compared to the solution spectra. Solid-state *trans*-PEP exhibits an absorption band at $\lambda =$ 361 nm due to non-associated pyrene units (compared to 346 nm in solution) with a cut off at $\lambda = 872$ nm (800 nm in solution). On the other hand, *cis*-PEP exhibits an absorption band at $\lambda = 356$ nm (349 nm in solution) with cut-off at 848 nm (747 nm in solution). The red shift can be attributed to an increased degree of conjugation occurring in both solid-state polymers, due to increased alignment and stacking of the pendant groups. Also, the well-defined band at $\lambda = 580$ nm observed for *trans*-PEP in solution ($\lambda =$ 590 nm in solid state) and that at $\lambda = 440$ nm for *cis*-PEP ($\lambda = 485$ nm in solid state) exhibit a large broadening upon attaining the solid state. This can be explained in terms of physical aggregation resulting from pyrene–pyrene intermolecular interactions between neighboring polymer chains.

3.2.2. Fluorescence spectra of trans-PEP and cis-PEP

Fluorescence spectra of the polymers in THF solution are shown in Fig. 6. The fluorescence spectrum of *trans*-PEP shows an emission band in the 360–465 nm region due to non-associated pyrene groups (also named 'monomer emission'). Apparently, no excimer emission is observed

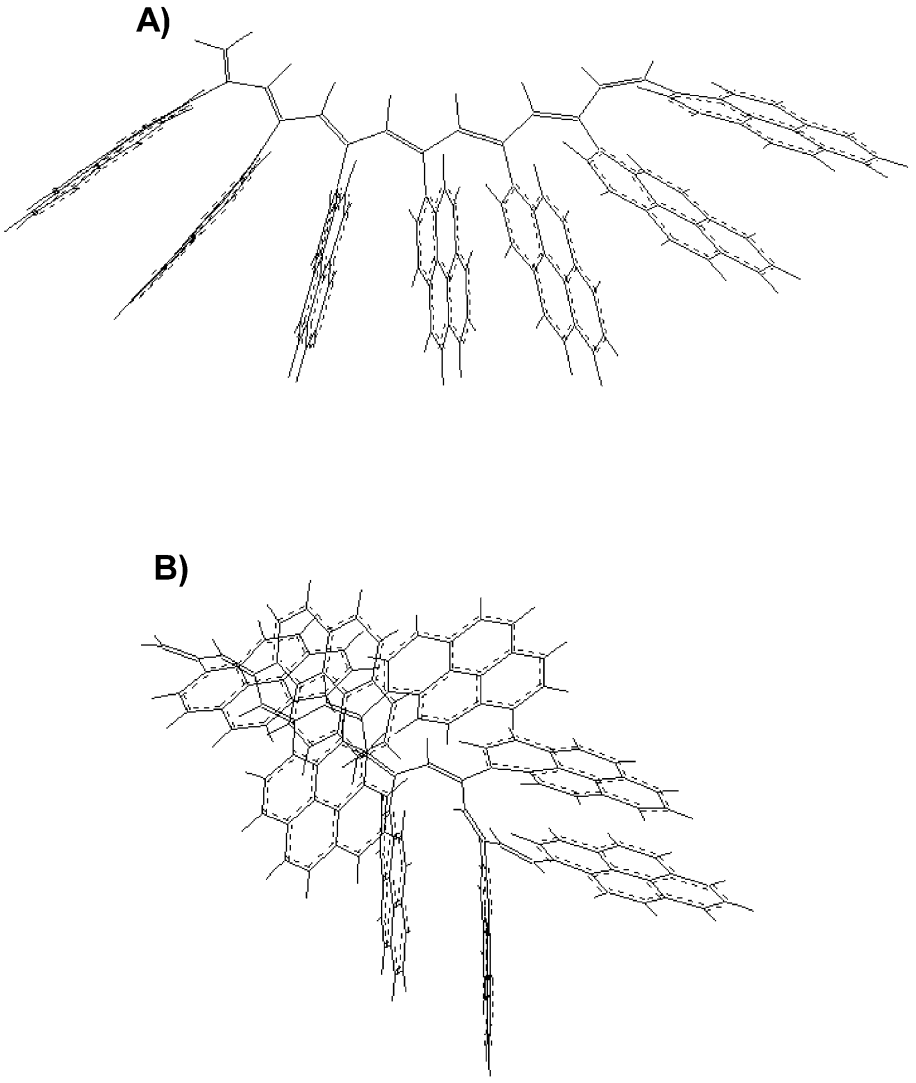

Fig. 5. Modeling structure for (A) *trans*-PEP and (B) *cis*-PEP in THF.

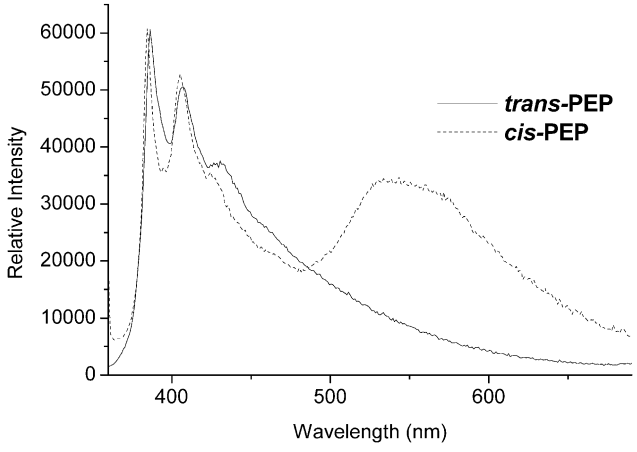

Fig. 6. Fluorescence spectra of *trans*-PEP *cis*-PEP in THF.

for this polymer. However, it is worth noting that there is an important emission intensity near 500 nm, a wavelength where pyrene itself does not emit, which reveals the presence of excited pyrene–pyrene complexes in *trans*-PEP.

By contrast, the fluorescence spectrum of *cis*-PEP shows two distinct bands (Fig. 6). The first emission band, with vibronic peaks, is very similar to that observed for *trans*-PEP and comes from excited non-associated pyrenes. The broad band around 550 nm results from intramolecular interactions between adjacent pyrene units along the molecular frame. Similar spectral properties were observed in the fluorescence spectrum for *syn*-di(1-ethynylpyrene) (DEPS) (Fig. 8). However, in this dimer, the excimer emission band appears at $\lambda_F = 482$ nm because of its dissimilar backbone configuration and lower conjugation length. Indeed, pyrene–pyrene intramolecular interactions are remarkably favored by a coiling of the twisted polyacetylene backbone in *cis*-PEP (Fig. 5(B)). Therefore, pyrene groups aggregate in a non-parallel way, thereby

interacting at shorter distances, which causes a red shift of the excimer emission band.

3.2.3. Excitation spectra of trans-PEP and cis-PEP

Excitation spectra of *trans*-PEP (Fig. 7(A)) and *cis*-PEP (Fig. 7(B)) recorded at λ_F of the 'monomer emission' (λ_F = 404 nm) and at λ_F of the excimer emission (λ_F = 480 nm for *trans*-PEP, λ_F = 560 nm for *cis*-PEP) are very different, which does not coincide with the rule of formation of a dynamic excimer [31]. Fluorescence lifetime decay profiles of *trans*-PEP and *cis*-PEP (not shown) recorded at λ_F of the 'monomer emission' and at λ_F of the excimer emission did not show any rising component. Corresponding excitation spectra, with time dependent fluorescence experiments showed that static excimer emissions take place in both polymers [36]. Thus, associations between adjacent pyrene pendant groups occur in the ground state of *trans*- and *cis*-PEP [31].

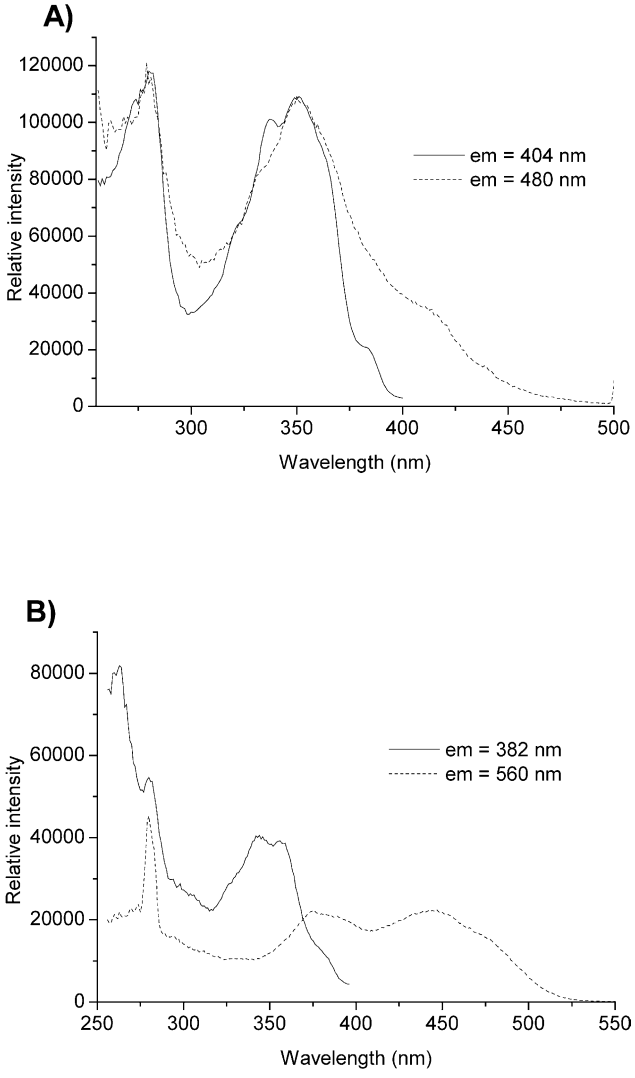

Fig. 7. Excitation spectra of (A) *trans*-PEP and (B) *cis*-PEP in THF.

3.2.4. Lifetime decay profiles of trans-PEP and cis-PEP

The average lifetimes measured at the fluorescence wavelength of the 'monomer emission' (λ_F = 404 nm) were $\langle\tau_F\rangle$ = 18.3 and $\langle\tau_F\rangle$ = 7.2 ns for *trans*-PEP and *cis*-PEP, respectively. Lifetimes for the static excimer emissions were remarkably shorter, about $\langle\tau_F\rangle$ = 8.4 ns (λ_F = 404 nm) for the former and $\langle\tau_F\rangle$ = 1.5 ns (λ_F = 506 nm) for the latter [36]. It is typically expected that the fluorescence lifetimes of excited non-associated pyrenes is higher [38], however, Borgig and co-workers reported that some pyrene monomers grafted to polyethylene exhibited similar short fluorescence lifetimes, about $\langle\tau_F\rangle$ = 13.3 ns [39].

The average fluorescence lifetime at λ_F of the 'monomer emission' is shorter in the *cis*-polymer, which confirms that pyrene–pyrene complexes in *cis*- and *trans*-PEP have different geometries as predicted by MM2 calculations (Fig. 4). In addition, the average lifetime measured for *cis*-PEP at λ_F = 560 nm is much shorter than that of *trans*-PEP at λ_F = 480. We think that the pyrene–pyrene complexes in *cis*-PEP are stronger and more stabilized.

3.3. Optical properties of the polymers and the model dimers

The main goal of this work is to investigate the nature of the complexes present in *trans*-PEP and *cis*-PEP, and to see how the geometry of the polymer backbone contributes to the modification of the polymer emission spectra. For that, we studied the optical properties of three model di(1-ethynylpyrene)s bearing all possible pyrene–pyrene arrangements. The structures of these compounds are shown in Fig. 2. Absorption spectra of DEPS, DEPA and DEPH (not shown) are very similar and exhibit a well-structured band at λ = 346 nm due to the S_2 excited state of pyrene groups.

Fluorescence spectra of DEPS, DEPA and DEPH are shown in Fig. 8. As we can see, all of these dimers exhibit broad emission bands in the 360–460 nm region due to excited non-associated pyrenes. DEPS also showed a very

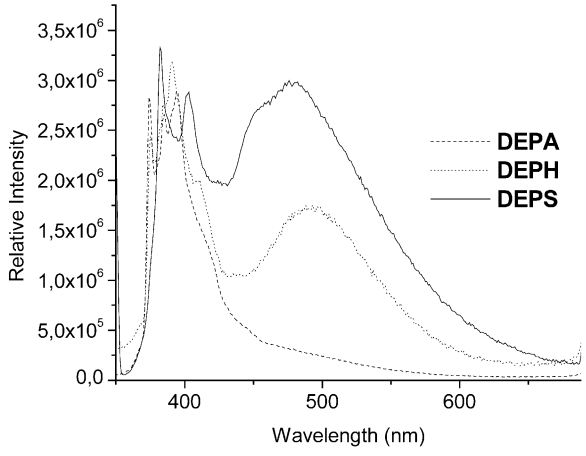

Fig. 8. Fluorescence spectra of DEPS, DEPA and DEPH in THF.

intense excimer emission band at $\lambda_F = 480$ nm, arising from intramolecular interactions between adjacent pendant pyrene groups. This dimer possesses a rigid butadiene main chain where both pyrene groups are situated on the same side of the backbone. The rigidity of the chain restrains their mobility, forcing pyrenes to stack. On the other hand, DEPH shows a similar 'monomer emission' followed by an excimer emission band at $\lambda_F = 498$ nm, which reveals the formation of an intramolecular pyrene–pyrene complex. Since, DEPH pyrenes are linked by an aliphatic chain, they have no mobility restrictions and can rotate freely. Therefore, the excimer emission of this dimer demonstrates that pyrene groups have a natural tendency to stack, resulting in stable pyrene–pyrene complexes.

Unlike DEPS and DEPH, DEPA shows no emission originating from an excimer complex. This can be explained in terms of geometry: the pyrene chromophores in DEPA are located on opposite sides of the rigid butadiene backbone, which prohibits them from interacting together. Intensity ratios (I_M/I_E) between the 'monomer emission' band (I_M) and the excimer emission band (I_E) were $I_M/I_E = 0.96$ and 1.84 for DEPS and DEPA, respectively. According to these results, and based upon arguments related to stereochemistry and the distances between pyrene groups we can assume that the complex formed in DEPS is stronger than that formed in DEPA as expected.

Another interesting point is that the fluorescence spectrum of DEPS shows an intense excimer emission band at $\lambda = 480$ nm, whereas *trans*-PEP shows only moderate emission at this wavelength. We think this is due to an energy transfer from the excited pyrene–pyrene complex to the highly conjugated polyacetylene backbone in *trans*-PEP. Further excitation spectra and time dependent fluorescence experiments confirmed the presence of static excimers in both DEPS and DEPH. This strongly indicates that pyrene–pyrene interactions in these dimers take place in the ground state [37].

3.4. Electrochemical properties and conductivity of the polymers

Conductivity (σ) of the polymers was measured in pressed pellet at room temperature in the non-doped state giving values of $\sigma = 2.7 \times 10^{-2}$ and 3×10^{-3} S/cm for *trans*-PEP and *cis*-PEP, respectively. These results are in agreement with those obtained from absorption spectra in the film (Fig. 4(B)) and suggest that the *trans*-polymer is more conjugated than its homologue *cis*-PEP (Fig. 5). As we can see, the conductivity values are quite different, which can be explained in terms of packing. The difference in conjugation length between *trans*-PEP and *cis*-PEP decreases in the solid state because the polyacetylene backbone of both polymers adopt a better aligned conformation. This can be detected by red shifts of the bands in the absorption spectrum (Fig. 4(B)). In the pressed pellet, the packing is tighter than in film, so that distance between neighboring polymer chains is reduced. Thus, electrical conduction can occur along the polymer backbone in an intermolecular fashion.

The electrochemical behavior of *cis*- and *trans*-PEP has been investigated by cyclic voltammetry [40–42] on a platinum disk electrode using a 0.1 M n-Bu_4NClO_4/THF solution as electrolytic medium and employing a detection scan rate of 10 mV/s. All potentials were measured with respect to an Ag/AgCl reference electrode.

Cyclic voltammograms of *cis*-PEP (Fig. 9(A)) and *trans*-PEP (Fig. 9(B)) showed irreversible potential waves located at 1.085 and 1.5 V, respectively. These result from the oxidation of the aromatic rings to give the corresponding cation-radicals. On the second scan, *cis*-PEP also showed a very discrete cathodic shoulder at 0.97 V. Both peaks in *cis*-

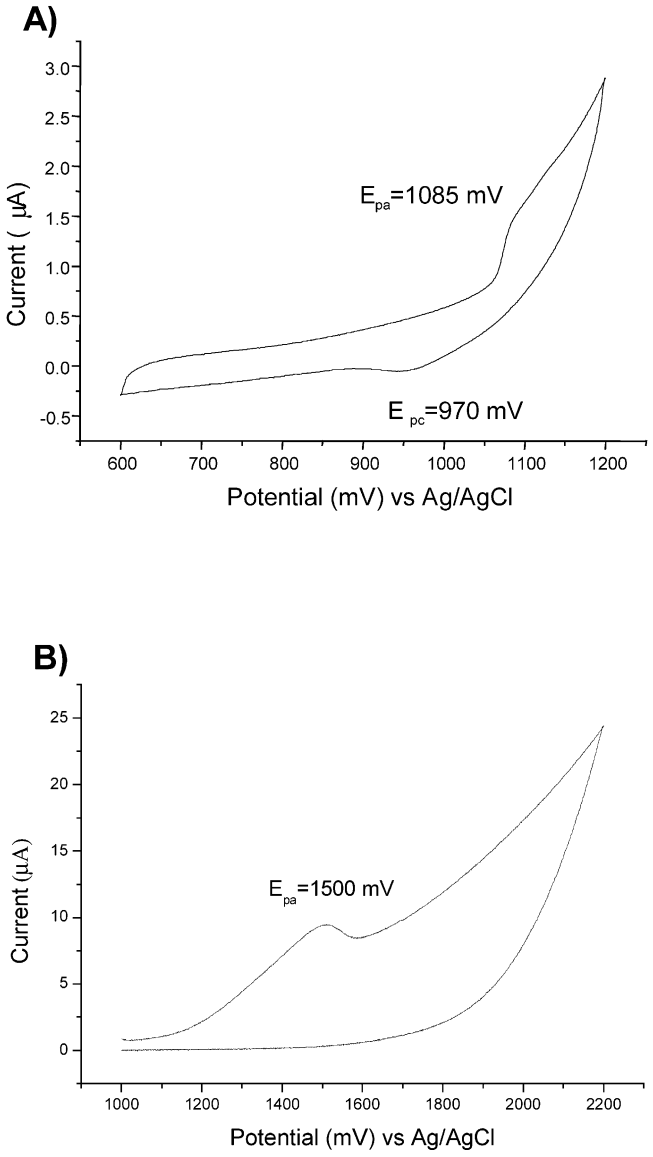

Fig. 9. Typical cyclic voltammogram for (A) *cis*-PEP 0.16 mM, and (B) *trans*-PEP 0.21 mM in 0.1 M n-Bu_4NClO_4/THF, platinum disk (0.0078 cm^2) as working electrode, scan rate 0.02 V s^{-1}.

PEP presented small current values (i_{pa} and i_{pc}) due to the reduced degree of conjugation in this polymer. This observation is supported by the fact that the absorption spectrum of *trans*-PEP shows an absorption band at 580 nm arising from the well-aligned polyacetylene backbone whereas *cis*-PEP shows only a shoulder at 537 nm due to the twisted polyacetylene main chain; increased polymer conjugation in *trans*-PEP suggests an increased stability which reduces the polymer's susceptibility to oxidation. The oxidation of *trans*-PEP gives rise to the formation of a cation-radical, which is highly stabilized by resonance and which is very difficult to reduce. By contrast the oxidation of twisted *cis*-PEP generates a cation-radical, which is less stabilized due to the reduced degree of conjugation and allows for further reduction of this polaron.

Anodic waves as those present in the cyclic voltammograms of the polymers were also observed for pyrene (Fig. 10(A)) and 1-ethynylpyrene (Fig. 10(B)). These compounds show irreversible anodic peaks at 1.35 and 1.58 V, respectively, due to the formation of cation-radicals. The generation of similar polarons by anodic oxidation of aromatic rings such as electrochemical oxidation of substituted naphthalenes [43] in protic solvents and dibenzo[*a*, *l*]pyrene in aprotic media [44] is already reported in the literature.

cis- and *trans*-PEP do not show a cathodic peak correlated to the observed anodic peaks, which suggests them to be conducting polymers. The big difference in electrochemical behavior originates from their dissimilar geometry.

In order to compare chemically prepared *cis*- and *trans*-PEP with an electrochemically prepared polymer, we carried out the electrolysis of 1-ethynylpyrene (2 mM) dissolved in a 0.1 M *n*-Bu_4NClO_4/THF solution at a controlled potential of 1.6 V [45]. The electrodeposited product passivated the anode, which was cleaned from time to time. Electrolysis was stopped after having passed 10.02 C over a 35 h period and the obtained product was a yellowish powder, which was characterized by ^{1}H NMR and UV–vis spectroscopy. The resulting oligomer of 1-ethynylpyrene was analyzed by cyclic voltammetry (Fig. 11) and exhibited electrochemical behavior similar to that of *trans*-PEP (Fig. 9(B)), with an irreversible anodic wave at 1.5 V. Unfortunately, it was not possible to obtain a high molecular weight polymer by electrochemical methods, probably due to the high steric effect of the monomer. Since, the oligomer electrochemically synthesized was obtained in the doped state, due to the electrolyte, it was not possible to compare its fluorescence spectrum with that of DEPS. Nevertheless, the cyclic voltammograms suggest that the oligomer geometry resembles that of *trans*-PEP. This is an indication that the *trans* configuration is favored in the electrochemical polymerization of 1-ethynylpyrene.

4. Conclusion

Thermal properties of *trans*-PEP and *cis*-PEP were determined by TGA and DSC. *trans*-PEP exhibited higher thermal stability than its homologue, *cis*-PEP. On the other hand, *trans*-PEP shows a softening point of $T_s = 330\,^{\circ}C$ whereas *cis*-PEP shows neither a softening point nor melting point in the studied range of temperatures.

The optical properties of *trans*-PEP and *cis*-PEP in THF solution were studied by UV–vis and fluorescence spectroscopy. *trans*-PEP possesses a higher effective degree of conjugation than *cis*-PEP. Both polymers show emissions originating from excited non-associated pyrene units and static excimers. Excitation spectra in conjunction with fluorescence decay profiles, measured at the wavelength of both fluorescence bands, proved that pyrene–pyrene intramolecular interactions (static excimers) are responsible for the observed long wavelength emissions. The long wavelength fluorescence band of *cis*-PEP indicates that pyrene

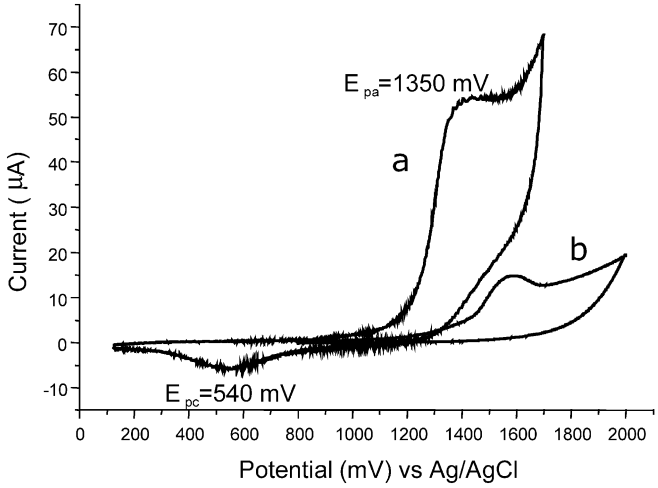

Fig. 10. Cyclic typical cyclic voltammogram for (A) pyrene 1 mM, and (B) EP 1 mM in 0.1 M *n*-Bu_4NClO_4/THF, platinum disk (0.0078 cm^2) as working electrode, scan rate 0.02 V s^{-1}.

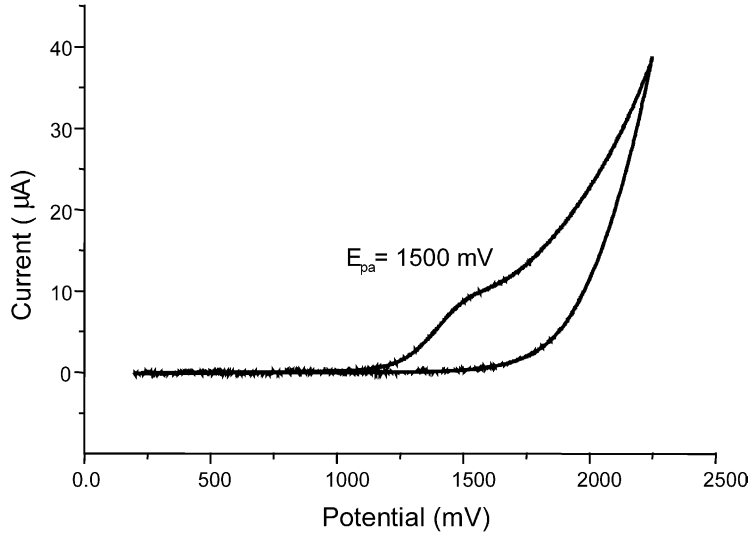

Fig. 11. Cyclic voltammogram for a saturated solution of the obtained oligomer in 0.1 *n*-Bu_4NClO_4/THF, platinum disk (0.0078 cm^2) as working electrode, scan rate 0.02 V s^{-1}.

units are closer to each other in this polymer and interact in a non-parallel way.

Fluorescence experiments carried out in model dimers confirmed that it is necessary for pyrene units to be on the same side of the polymer backbone to generate a static excimer emission. The presence of double bonds restrains the mobility of pyrene units, favoring the formation of complexes. However, when two pyrenes are linked by a saturated propane chain, the aromatic groups have a natural tendency to stack. The electrochemical behavior of both polymers was very different, which agrees with their optical properties and conductivity values. Electrochemical polymerization of 1-ethynylpyrene lead to the formation of an oligomer with *trans* geometry.

Acknowledgements

We thank Prof Gilles Durocher and Dr Michel Belletête of the Université de Montréal for their assistance with steady state and lifetime fluorescence spectra. We are also grateful to Miguel Angel Canseco for his help with TGA and DSC measurements. This work was financially supported by NSERC-Canada and IIM-UNAM. JABM is grateful to CONACyT and DGEP-UNAM for doctoral and complementary fellowships, respectively.

References

[1] Friend RH, Gymer RW, Holmes AB, Burroughes JH, Marks RN, Taliani C, et al. Nature 1999;397:121–8.
[2] Heeger AJ. Angew Chem, Int Ed Engl 2001;40:2591–611.
[3] Segura JL, Martin N. J Mater Chem 2000;10:2403–35.
[4] Kraft A, Grimsdale AC, Holmes AB. Angew Chem, Int Ed Engl 1998; 37:402–28.
[5] Bernius MT, Inbasekaran M, O'Brien J, Wu WS. Adv Mater 2000;12: 1737–50.
[6] Chien JCW. Polyacetylene. New York: Academic Press; 1984.
[7] Gingsburg EJ, Gorman CB, Grubbs RH, Stang PJ, Diederich editors. Modern acetylene chemistry. New York: VCH; 1995.
[8] Shirakawa H, Masuda T, Takeda K, Patai S. The chemistry of triple bonded functional groups supplement C2. New York: Wiley; 1994 [chapter 17].
[9] Schrock RR. Acc Chem Res 1990;23:158–65.
[10] Masuda T, Higashimura T. Adv Polym Sci 1987;81:121.
[11] Tang BZ, Poon WH, Leung SM, Leung WH, Peng H. Macromolecules 1997;30:2209–12.
[12] Simionescu CI, Percec VJ. Polym Sci Polym Symp 1980;67:43–71.
[13] Simionescu CI, Percec VJ, Dumitrescu SJ. Polym Sci, Polym Chem Ed 1977;15:2497–509.
[14] Masuda T, Tavhimori HJMS. Pure Appl Chem 1994;A31:1675–90.
[15] Masuda T, Karim SMA, Nomura R. J Mol Catal A 2000;160:125–31.
[16] Karim SMA, Musikabhuma K, Nomura R, Masuda T. Proc Jpn Acad Ser B 1999;99:7.
[17] Tang BZ, Kong X, Wan X, Feng XD. Macromolecules 1997;30: 5620–8.
[18] Shimizu T, Yamamoto T. Inorg Chim Acta 1999;296:278–80.
[19] Shimizu T, Yamamoto T. Chem Commun 1999;6:515–6.
[20] Mastrorilli P, Nobile CF, Rizzuti A, Suranna GP, Acierno D, Amendola E. J Mol Catal A 2002;178:35–42.
[21] Piçarra S, Relogio P, Alfonso CAM, Martinho JMG, Farinha JPS. Macromolecules 2003;36:8119–29.
[22] Duhamel J, Kanagalingam S, O'Brien TJ, Ingratta MW. J Am Chem Soc 2003;125:12810–22.
[23] Mizayazawa K, Winnik FM. J Phys Chem B 2003;107:10667–82.
[24] Pandey S, Redden RA, Fletcher KA. Macromol Chem Phys 2003;204: 425–35.
[25] Berglund KD, Przybycien TM, Tilton RD. Langmuir 2003;19: 2705–13.
[26] Beaudoin E, Hiorns RC, Borisov O, François J. Langmuir 2003;19: 2058–66.
[27] Gao C, Qian H, Wang SJ, Wei Chen DY, Yu G. Polymer 2003;44: 1547–52.
[28] Morimoto H, Hashidzume A, Morishima Y. Polymer 2003;44: 943–52.
[29] Yusa S, Sakakibara A, Yamamoto T, Morishima Y. Macromolecules 2002;35:10182–8.

[30] Ellison CJ, Torkelson JM. J Polym Sci, Part B: Polym Phys 2002;40: 2745–58.
[31] Winnik FM. Chem Rev 1993;93:587–614.
[32] Rivera E, Belletête M, Zhu XX, Durocher G, Giasson R. Polymer 2002;43:5059–68.
[33] Rivera E, Wang R, Zhu XX, Zargarian D, Giasson R. J Mol Catal A 2003;204-205:325–32.
[34] Tabata M, Sone T, Sadahiro Y. Macromol Chem Phys 1999;200: 265–82.
[35] Wang R, Bélanger-Gariépy F, Zargarian D. Organometallics 1999;18: 5548–52.
[36] Belletête M, Rivera E, Giasson R, Zhu XX, Durocher G. Synth Met 2004;143:37.
[37] Rivera E, Belletête M, Winnik FM, Giasson R, Durocher G. Manuscript in preparation.
[38] Nijegorodov NI, Downy WS. J Phys Chem 1994;98:5639–43.
[39] Danko M, Hrdlovic P, Borsig E. J Macromol Sci-Pure Appl Chem 2001;A38:467–86.
[40] Heinze J. Angew Chem, Int Ed Engl 1984;831.
[41] Evans DH. Acc Chem Res 1997;10:313.
[42] Kissinger PT, Heineman WR. J Chem Ed 1983;9:702.
[43] Utley JHP, Rozenberg GG. Tetrahedron 2002;58:5251.
[44] Li KM, Byun J, Gross ML, Zamzow D, Jankowiak R, Rogan EG, et al. Chem Res Toxicol 1999;12:749.
[45] Bard AJ, Faulker LR. Electrochemical methods. Fundamentals and applications. New York: Wiley; 1980 [chapter 10].